Towards phosphorus recycling for agriculture by algae: soil incubation and rhizotron studies using ^{33}P-labeled microalgal biomass

Nina Siebers[a*], Diana Hofmann[a], Henning Schiedung[a.b**], Alexander Landsrath[b], Bärbel Ackermann[c], Lu Gao[c], Peter Mojzeš[c,d], Nicolai D. Jablonowski[c], Ladislav Nedbal[c], and W. Amelung[a.b]**

[a] *Forschungszentrum Jülich GmbH, IBG-3: Agrosphere, 52428 Jülich, Germany*

[b] *Institute of Crop Science and Resource Conservation, Soil Science and Soil Ecology, Nussallee 13, University of Bonn, 53115 Bonn, Germany*

[c] *Forschungszentrum Jülich GmbH. IBG-2: Plant Sciences, 52428 Jülich, Germany*

[d] *Institute of Physics, Faculty of Mathematics and Physics, Charles University, CZ-12116 Prague 2, Czech Republic*

* Corresponding author: n.siebers@fz-juelich.de, Tel.: +49 (0)2461 61 96614

** Equal contributing authors

Abstract

Algae effectively accumulate phosphorus (P) from the environment, qualifying them as a promising novel P fertilizer. We hypothesized that P in algae can be rapidly transformed in soil and mobilized for plant growth. To determine the fate of algal fertilizer in soil and to trace its efficiency for plant uptake, we labeled the algae *Chlorella vulgaris* with the radioisotope ^{33}P. To optimize the labeling we studied P-uptake dynamics in detail using a pre-starved culture and additionally monitored polyphosphate (Poly-P) and organic carbon (C) reserve pools by Raman microscopy. Using an optimized labeling procedure, the concentrations and distribution of both algae-derived ^{33}P and mineral fertilizer ^{33}P (control) were characterized in incubation and rhizotron experiments. Soil incubation was performed with four major reference groups (Andosol, Alisol, Cambisol, and Vertisol). To assess ^{33}P plant uptake we grew wheat in rhizotrons on Cambisol. Soil analyses at different incubation times demonstrated sequential ^{33}P fractionation, while plant uptake of algae-derived ^{33}P was followed using sequential autoradiographic imaging. We found that the algae increased labile P pools comprising Resin- and $NaHCO_3$-extractable P in soils during the first 2 weeks of incubation, similar to the effects of NPK fertilizer. The soils with elevated concentrations of Fe- and Al-oxides (Andosol and Alisol) immediately bound 55 to 80% of the applied fertilizer ^{33}P into the moderately available NaOH-P fraction, whereas the soils with lower concentrations of Fe/Al-oxides (Cambisol, Vertisol) stored 35-71% of the algal-P in the labile fraction. The rhizotron experiments visually supported the release and plant-uptake of algal ^{33}P, thus verifying the suitability of algal-fertilizer for plant growth.

Keywords: *Chlorella vulgaris*; sequential P fractionation; autoradiography; wheat; ^{33}P labeling

1 Introduction

Phosphorus (P) is an essential element for all organisms and plants. Besides nitrogen (N), P is the most important fertilizer in agriculture (Scholz et al., 2013). Rock phosphate ─ a non-renewable resource ─ is the major raw material for production of mineral P fertilizer. About 80% of the annual mined phosphate rock is used in agriculture (Scholz et al., 2013), making it one of the key resources for maintaining food security for the continuously growing world population. There are considerable uncertainties on how long residual rock phosphate reserves may still support global requirements, with estimates ranging between 40 to 400 years (Obersteiner et al., 2013). In either scenario phosphate rock remains a limited, non-renewable resource. Additional concerns relate to contamination of rock phosphates with cadmium and uranium and to their occurrence in politically unstable regions (Vaccari, 2009; Reijnders, 2014). Natural geochemical P cycling requires millions of years, so it is essential to capture P from waste streams close to their source and return this nutrient to agriculture in form of novel P fertilizers. Algae are promising in this regard, because they can rapidly acquire P from natural eutrophic water bodies (Mainstone and Parr, 2002; Wallmann, 2010) and from wastewater (Aslan, et al., 2006). Optimizing algal P uptake from P rich waste and re-using the algal biomass as a fertilizer for agricultural production might thus help overcoming many of future limits in P fertilizer supply.

Microalgae are capable of accumulating P in reserves substantially larger than requirements for their immediate growth (Brown and Shilton, 2014). This capacity evolved to cope with episodes of P starvation that frequently occur in nature. Often, P reserves in algal cells occur as Poly-P (Stewart, 1974; Nishikawa et al., 2006), which has already found use as industrial fertilizer (McBeath et al., 2007). Overall, microalgal biomass may contain up to several weight percent P (Powell et al., 2009; Solovchenko et al., 2016; Whitton et al., 2016). In addition to P, algae

accumulate reserves of other macronutrients such as N and K from waste streams (Ruiz et al., 2011).

To be used as a fertilizer for agricultural production, algal biomass must be transformed in soil to chemical forms that are available for uptake by plant roots. The polysaccharide and glycoprotein matrix of algal cell walls can provide a strong defense against the ambient environment, as reported, e.g., for the microalga *Chlorella emersonii* (Afi et al., 1996; Fleurence, 1999; Gerken et al., 2013). The *C. vulgaris* cell wall does not consist of a resistant, trilaminar outer cell wall of aliphatic, non-hydrolysable macromolecules (Afi et al., 1996) as does *Chlorella emersonii*, but is also an effective mechanically barrier. These properties may delay nutrient release, thus qualifying algal biomass as potential slow release fertilizer, with the additional benefit of limiting conversion of algal P into biologically inaccessible forms, a process occuring particularly in Al- or Fe-rich soils. However, mineralization of algal biomass should be fast enough to provide nutrients for plant growth. It is thus important to ask whether particularly biotechnologically relevant, fast growing microalgae, such as those of the genus *Chlorella,* can release sufficient P for plant nutrition when used as a fertilizer. This capability has been demonstrated in plant-growth experiments (Schreiber et al., 2018) but needs to be tested in broader spectrum of soil types.

To evaluate the degradation of algal biomass in soils and to study the bioavailability and uptake of this recycled P into plants, chemical differentiation between algae-derived P and P occurring in natural soil types is necessary. Here we used the radioisotope ^{33}P, to trace P from algal biomass into soil and finally into plants, visualized by autoradiographic imaging of plant roots and shoots in rhizotrons (Bauke et al., 2017).

Raman microscopy is a convenient tool to monitor accumulation of Poly-P reserves in microalgal cells (Moudříková et al., 2017). Poly-P can be clearly recognized by its unique

Raman spectrum, and quantified in a label-free manner even in the presence of other biomolecules (Moudříková et al., 2016). The Raman signal has been shown to be a good linear proxy for the much more time-demanding enzymatic assay (Moudříková et al., 2017). Here, Raman microscopy was used to optimize the protocols for ^{33}P labeling of Poly-P in algal cells.

This study aimed at (i) characterizing P release from algae and its transformation into biologically accessible chemical forms in common agricultural soils, and (ii) at assessing the fertilizing effect of algal biomass for wheat growth. To accomplish these goals, we labeled *Chlorella vulgaris* with ^{33}P, studied the ^{33}P release from the algal biomass in four reference soil groups (Andosol, Alisol, Cambisol, Vertilsol) via an incubation experiment, and imaged the uptake of ^{33}P from algae in soil into wheat (*Triticum aestivum*) via a rhizotron experiment.

2 Material and Methods

2.1 Algae cultivation and ^{33}P-labeling

Chlorella vulgaris IPPAS C1 was obtained from the culture collection of the K.A. Timiryazev Institute of Plant Physiology (IPPAS), Russian Academy of Science (courtesy of M. Sinetova). *Chlorella vulgaris* CCALA265 was purchased from the culture collection of the Botanical Institute, Trebon, Czech Republic. The growth medium was prepared as described in Brányiková et al. (2011) and consisted of the following in mM: 18.32 $(NH_2)_2CO$, 1.74 KH_2PO_4, 0.83 $MgSO_4 \times 7H_2O$, 0.79 $CaCl_2$, 0.11 FeNa-$C_{10}H_{12}O_8N_2$, 0.017 $MnCl_2 \times 4H_2O$, 0.013 H_3BO_3, 0.009 $ZnSO_4 \times 7H_2O$, 0.004 $CuSO_4 \times 5H_2O$, 0.002 $CoSO_4 \times 7H_2O$, 0.0001 $(NH_4)_6Mo_7O_{24} \times 4H_2O$ and 0.0001 $(NH_4)VO_3$ made up in deionized water.

Cultivations for later radioactive labeling were done in the FMT150 photobioreactors (PSI, Brno, Czech Republic) as described in Nedbal et al. (2008). All experiments were done with five replicates (n=5). The cultures were incubated at 35 °C, which was found to be the optimum

113 temperature (data not shown), at pH 7–8, at saturating irradiance levels of 2200 µmol
114 (photons)·m^{-2}·s^{-1} generated equally by sets of red and blue light emitting diodes. Cultures were
115 first incubated for 3 days in a batch in complete medium to eliminate any influence of culture
116 history and to standardize for reproducibility of initial culture properties. Subsequently, the algae
117 were harvested by centrifugation and re-suspended in growth medium described above but
118 without KH_2PO_4. Culture dynamics in P-free medium were determined by automated
119 measurement of optical density in the photobioreactor until growth ceased. P-limitation was then
120 confirmed by demonstrating that orthophosphate addition restores growth.
121 In preliminary experiments with two replicates, we found that efficient P-labeling requires at
122 least a minimum P concentration; for this purpose we added 10 µL of a 680 µM ^{33}P solution to
123 the algae cultures described above. To ensure that at the end the algae contain sufficient quantity
124 of P for plant growth but to avoid that all of this P is radioactive and thus potentially toxic, we
125 continued P uptake experiments by additionally adding 120 µL of non-radioactive P solution in
126 the flask.
127 To prepare for ^{33}P labeling. algal growth dynamics after adding different concentrations of
128 orthophosphate were either monitored to follow the uptake dynamics (Figure 1) or to observe
129 polyphosphate accumulation (Figure 2). P-starved algae were labeled with ^{33}P by transferring the
130 equivalent of 0.51 g algal biomass (dry weight) in 50 mL medium into Erlenmeyer flasks to
131 which 870 kBq $^{33}PO_4^{3-}$ (Hartmann Analytic GmbH, Braunschweig) was added. These flasks
132 were sealed with wadding plugs to prevent liquid from spilling out and to reduce evaporation,
133 placed on an orbital shaker in a temperature-controlled growth chamber and exposed to a weak
134 warm white light of 200 µmol (photons)·m^{-2}·s^{-1} to support photoautotrophic growth for up to 4
135 days. All treatments were conducted with two replicates. Preliminary experiments had shown
136 that prolonging algal growth beyond 4 days did not improve ^{33}P uptake.

Radionucleotide uptake was monitored by taking aliquots of the culture and pelleting the algal cells by centrifugation at 12,500 × *g* for 20 min. To determine $^{33}PO_4^{3-}$ activity in the supernatant we carefully removed the top half of it and measured it with a liquid scintillation counter (LSC) as described in Bauke et al. (2017). The pellets were washed several times using 50 mL deionized water in order to remove all ^{33}P that was not incorporated within the algal cells. The supernatant of each washing step was also analyzed by LSC. The final algae pellets were digested using 4 mL concentrated HNO_3 at 180 °C for 6 h prior to LSC analyses for which 10 mL aliquots were mixed with 10 mL LSC cocktail (ULTIMA Gold, PerkinElmer, Solingen, Germany) and subsequently measured by a Tri-Carb® 3110TR LSC counter (PerkinElmer, Solingen, Germany). These experiments showed that 66 and 99% of initially supplied ^{33}P was incorporated in algal cells in the two cultures, respectively. At the end of the cultivation period, labeled algae were then centrifuged at 12500 ×g for 20 min, and washed once using deionized water to remove ^{33}P that was not incorporated within the algae. Labeled biomass was dried at 40 °C for 48 h and ground in a mortar for soil incubation experiments and used in suspension for rhizotron experiments. The algae contained 47.6±0.0% C; 9.6±0.0% N, and 1.4±0.1% P (n=6).

Labeled mineral fertilizer was prepared in triplicate by mixing N (calcium ammonium nitrate), P (triple super phosphate; TSP), and K (potassium oxide) at the same proportions measured in the algal biomass. For the soil incubation experiment, prior to mixing the three single components we labeled the TSP with ^{33}P using 6.1 MBq $^{33}PO_4^{3-}$ added to 22 mg TSP that was dissolved in 300 mL deionized water. This labeled TSP solution was dried in an oven at 60 °C for 3 days, allowing the TSP to recrystallize. Finally, the crystals were ground for an evenly distribution of ^{33}P and applied to the soil as NPK fertilizer. The concentration measured by ^{33}P activity was 1736±76 Bq g^{-1} soil.

2.2 Imaging polyphosphate reserves by Raman microscopy

Raman microscopy was used to identify the dynamics of Poly-P accumulation and to determine when to harvest cells having high Poly-P. Specimen preparation for Raman measurements, the experimental workflow, and the data analysis methodology are described in detail in Moudříková et al. (2017). Briefly, harvested algal cells were immobilized in 1% w/v solution of low-gelling agarose (T = 39 °C), spread between a quartz slide and coverslip, and sealed with a CoverGrip sealant (Biotium) to prevent cell movement and evaporation of water during the course of observations.

Raman maps were acquired using a confocal Raman microscope (WITec alpha300 RSA, WITec, Germany), an oil-immersion objective (UPlanFLN 100×, NA 1.30, Olympus, Japan), and 532 nm excitation (20 mW power at the objective focal plane). The scanning step in in the *x* and *y* directions was 220 nm, with an integration time of 0.1 s per pixel. Acquisition of a Raman map for a single cell of the size of *Chlorella vulgaris* CCALA256 requires about 150 s. To prevent chlorophyll autofluorescence, a wide-area, low-power photobleaching was applied prior to the mapping, as described previously (Moudříková et al., 2016).

For each sample, Raman maps of 30 – 50 randomly chosen cells were acquired to capture the natural heterogeneity of the cultures. Figure 2 illustrates the transient Poly-P accumulation observed in four arbitrarily chosen pre-starved cells (blue) that occurred after addition of orthophosphate. Significant transient modulation of neutral lipids (red) and starch (green) accompanied the emergence of large Poly-P reserves. These observations demonstrated that two hours after adding orthophosphate, cells with large Poly-P depots are available for harvest.

2.3 Soil sampling and general characteristics

184 The potential for using algae as an alternative fertilizer may be particularly relevant in the tropics
185 or subtropics because uptake of P from wastewaters by algae is maximized with abundant solar
186 radiation and stable temperatures throughout the year. Therefore, we used samples from the
187 upper A horizon of a Vertisol (7.45°S, 111.61°E, 80 m a.s.l.), an Alisol (6.54°S, 106.52°E, 250
188 m a.s.l.), and an Andosol (6.88°S, 106.94E, 900 m a.s.l.) from the tropical island of Java,
189 Indonesia, as described in Winkler et al. (2016) and Lehndorff et al. (2016). All soils were
190 obtained from lands managed with upland crops. For comparison to a widespread soil group
191 typical of temperate climates, we additionally sampled the Ap horizon (0-10 cm) of a Cambisol
192 (WBR, 2015) from Germany (6.45°S, 50.87°E, 108 m a.s.l.). General soil characteristics are
193 shown in Table 1.
194
195 **2.4 Soil incubation experiments and analyses**
196 For incubation experiments, we used 15 g air-dried topsoil (0-30 cm) from each soil type,
197 adjusted the soil moisture to 50% water holding capacity (WHC) and introduced it to the lower
198 half of 250 mL Nalgene® vessels (Thermo Fisher Scientific, Waltham, Massachusetts, USA).
199 The vessels were not completely filled in order to maintain a sufficient reservoir for soil aeration,
200 and were opened twice a week for at least 1 h to compensate for oxygen consumption. Three
201 replicates of each soil type were prepared. Samples were pre-incubated at 25 °C for one week
202 prior to fertilizer addition. To ensure an equal distribution of the very small amount of ^{33}P-
203 labeled fertilizer in the soil, we homogenized the amount of fertilizer needed (corresponding to
204 an application rate of 35 kg P ha^{-1}) for each replicate in 1 g quartz sand and added this mixture to
205 the soil sample with a vortex mixer. Samples were then further incubated at 25 °C for 10 weeks.
206 After one, two, three, five, seven, and ten weeks of incubation, 0.5 g of dry soil equivalent was
207 sampled from each replicate (n=3), added to 50 mL centrifugation tubes, and sequentially

208 fractionated according to Hedley et al. (1982). Briefly, samples were serially treated with
209 solutions of increasing extractant strength: Resin (Resin-P), 0.5 M $NaHCO_3$ ($NaHCO_3$-P), 0.1 M
210 NaOH (NaOH-P), 1 M HCl (HCl-P), and Aqua regia (Residual-P). The ^{33}P activity of each
211 fraction was analyzed by LSC.
212
213 **2.5 Rhizotron experiments**
214 To support the soil incubation data by visualizing P uptake from algal fertilizer, we compared the
215 performance of ^{33}P-labeled algal fertilizer with ^{33}P-labeled conventional NPK fertilizer in a
216 rhizotron study using spring wheat (*Triticum aestivum* cv, Cornetto, S.G.L GmbH, Erftstadt-
217 Gymnich, Germany). For these experiments we used self-constructed rhizotrons, each built from
218 a black polyvinyl chloride (PVC) frame supporting a 10 mm thick transparent
219 polymethylmethacrylate (acrylic glass) plates, with a volume of 5.25 L (50 x 30 x 3.5 cm inner
220 dimensions).
221 To simulate top- and subsoil, rhizotrons were filled with a 30 cm layer of sand (RBS GmbH,
222 Inden, Germany; particle size: ≤ 1 mm) covered by a 10 cm layer of a 1:1 Sand:Cambisol (WBR,
223 2015) mixture, and finally a 5 cm layer of a 3:1 sand:Cambisol mixture. The Cambisol originates
224 from a P-depleted plot (no P fertilization since 1942) of the long-term experiment at a former
225 experimental research station of the University of Bonn at Dikopshof (50°48'27.8"N
226 6°57'10.8"E; as described in Mertens et al. (2008), and which was left over from a study by
227 Bauke et al. (2017). Both soils were air-dried at 40 °C for 5 days and passed through a 2 mm
228 sieve before introduction into the rhizotrons. After introduction into the rhizotrons each soil was
229 re-compacted to a bulk density of 1.4 g cm^{-3} and separately moisture-adjusted to 50% water
230 holding capacity and left for settlement for several days.

We performed four replicates of each treatment (algal and mineral fertilizer) , applying the equivalent of 35 kg P ha^{-1}, thus utilizing 8 rhizotrons. In contrast to the incubation experiment, we added the mineral fertilizer as a solution and the algal fertilizer as a suspension in 150 mL H_2O, again adjusting the N-P-K ratio of the mineral fertilizer to match the nutrient content of the algal fertilizer. This allowed us to test whether fresh algal fertilizer (with intact cell walls) can quickly release P in a plant-available form. In these experiments, the elemental content of the algae was 9.2% N, 2.6% P, and 1.1% K (m/m dry weight) and thus the applied amount of added algae equaled 1.4 g dry weight (0.2 g ^{33}P-labeled and 1.2 g non-labeled algae) per rhizotron. The fertilizer solution/suspension was applied on the upper soil layer, incorporated with a fork, and covered with a 5 cm thick layer of the topsoil to prevent the release of radiolabeled material to the air. Spring wheat seeds were pre-germinated for 3 days and one healthy seedling with three roots was planted in each rhizotron after fertilizer addition, 1 cm deep in the upper soil layer. Rhizotrons were then placed at an angle of 45° in a climate chamber with a day-length of 16 h and a light intensity of 320 µmol m^{-2} s^{-1} PAR. Day and night temperatures were set to 20 °C and 12 °C, respectively, at a relative air humidity of 60%.

2.6 ^{33}P imaging

For weekly ^{33}P imaging, the front plate of one rhizotron per treatment was opened to ensure direct contact between roots, shoots, and soil with the image plates (IPs). All IPs were covered with a thin protective foil to prevent contamination or damage by water or soil. In the first three weeks we used one large IP (35 x 43 cm, DÜRR NDT GmbH & CO, KG. Bietigheim-Bissingen, Germany), later combining images from a large IP (roots) and a small IP (20 x 40 cm, DÜRR NDT GmbH & CO, KG, Bietigheim-Bissingen, Germany) (plant) for each rhizotron. To ensure close contact between IPs and rhizotrons/wheat plants, the imaging assemblies were compressed

with small tungsten weights. The IPs on the soil surface and the shoots were exposed for 4 h. After exposure, the IPs were scanned in sensitive mode, with a resolution of 100 μm, using an Image Plate Scanner (CR35 Bio, Raytest, Germany).

No quantitative analysis of the ^{33}P activity was performed, nor was longer cultivation attempted because rhizotron cultivation was suboptimal and all treatments, including the control, developed fungal infestations with signs of the stem rust and reduced biomass productivity progressing with increasing time of growth.

2.7 Data treatment and statistical analyses

Statistical analyses were performed in SPSS (IBM SPSS Statistics, Version 22.0, Armonk, NY). We tested for normal distribution using the Shapiro-Wilk test ($P < 0.05$) and for homogeneity of variance using the Brown-Forsythe test ($P < 0.05$). To test for the effects of different fertilization treatments we performed one-way ANOVA. We considered the sampling times of the incubation study as paired samples. To account for this, we performed Repeated Measures ANOVA, with sampling times treated as repeated measures. If significant differences occurred we used the Tukey HSD test for post-hoc separation of means ($P < 0.05$). To test for the effect of fertilization within one sampling time, we performed a paired t-test separately ($P < 0.05$).

The evaluation software AIDA (AIDA Biopackage, Raytest, Germany), was used to convert the scans of the rhizotron images to rainbow-color images.

3 Results

3.1 Dynamics of growth, P-uptake, and ^{33}P labeling by starved algal culture

Addition of orthophosphate to the P-prestarved culture produced bi-phasic P uptake dynamics (Figure 1). Here, the fast component was shorter than the lag phase observed in the culture

279 growth. This fast uptake phase occurred during lag phase at both high and low orthophosphate
280 concentrations; always leading to a rapid transient accumulation of large P-reserves because the
281 cells were not growing during the lag phase.
282 In order to identify the chemical forms of the incorporated P, particularly Poly-P granules, We
283 performed Raman microscopy. These experiments utilized *Chlorella vulgaris* CCALA265,
284 whose cells are larger than the *C. vulgaris* IPPAS C1 cells used elsewhere in this study. These
285 larger *C. vulgaris* CCALA265 cells were easier to image than *C. vulgaris* IPPAS C1 without
286 having any effects on the dynamics of the Poly-P as confirmed by enzymatic analysis (Tabea
287 Mettler-Altmann, unpublished). No Poly-P granules were detected in the initial P-starved culture
288 (Figure 2, row A). Substantial Poly-P reserves were detected 2 h after adding orthophosphate
289 (Figure 2, row B), and during early exponential growth phase (Figure 2, row C). Rapidly
290 growing cells (Figure 2, row D) were typically somewhat smaller than lag phase cells and
291 contained only traces of polyphosphate and small amounts of starch and neutral lipids
292 representing organic C reserves. These experiments confirmed the effectiveness of our method
293 for rapid labeling of P-starved culture with ^{33}P. Based on the results shown in Figures 1 and 2 we
294 expect that a large proportion of added ^{33}P will be incorporated into Poly-P granules during lag
295 and early exponential phases, and that this P stored in form of Poly-P granules will subsequently
296 be used for cell growth after conversion to other chemical forms during prolonged cultivation.
297

298 **3.2 Sequentially extracted P fractions**

299 The different soil groups contained different distributions of P: total P concentration (P_t) is
300 described in Table 1 and was highest in the Andosol, at 1.9 times higher than in the Cambisol,
301 2.8 times higher than in the Alisol, and 6.1 times higher than in the Vertisol (Table 1). The
302 concentration of easily extractable P (Resin-P and $NaHCO_3$-P) was low in the Andosol, Alisol,

303 and Vertisol, but 10 to 17 times larger in the Cambisol. This trend was reversed for the NaOH-P
304 pool, especially for the Andosol; however, it was not as pronounced as for Resin-P and
305 $NaHCO_3$-P pools. The Residual P fraction contributed most to P_t with proportions ranging
306 between 42 to 70% (Table 1).
307 Due to the inhomogeneous distribution of the ^{33}P label within the TSP and the labeled algae, the
308 replicates and variants exhibited different initial ^{33}P activities (Supplementary Information, Table
309 S1). Thus, a direct comparison of ^{33}P activities between replicates and variants was not possible.
310 Therefore, we estimated the proportions of the ^{33}P activity in relation to the total ^{33}P activity
311 applied (Supplementary Information, Table S2). The typical ^{33}P distribution among the P
312 fractions was similar, whether it was delivered as NPK fertilizer or as algal biomass. The HCl-P
313 and Residual P pools received the lowest proportions of applied ^{33}P label (4 to 21% of the
314 applied amount), whereas label was distributed variably into the other fractions, i.e., Resin-P,
315 $NaHCO_3$-P, and NaOH-P (contributing between 12 and 82% of the applied ^{33}P (Figure 3,
316 Supplementary Information, Table S2). This large variation reflected the different ability of the
317 soils to bind P to its constituents, whereas the fertilizer form affected this P pool distribution less
318 drastically, and, intriguingly, not even consistently. Generally, the dissolution of NPK resulted in
319 larger ^{33}P activities in the Resin- and $NaHCO_3$-extractable P pools, particularly in the Cambisol
320 and Vertisol. In contrast, Algal fertilizer ^{33}P mainly accumulated in the NaOH-extractable P
321 pool, commonly described as moderately labile P (Negassa and Leinweber, 1996). The lowest
322 ^{33}P activities were found in the HCl-extractable P fraction (< 6% of applied ^{33}P), with
323 comparable contributions from the algal and the NPK fertilizers (Figure 3; Supplementary
324 Information, Table S2).
325 In respect to temporal trends, P release patterns were reflected in the changing proportions of ^{33}P
326 activity of sequential fractionation P-pools over time of the incubation. The trends in NPK and

algae treatments exhibited similar release patterns (Figure 3). In the Cambisol and Vertisol, the proportions of the Resin-P and $NaHCO_3$-extractable P fractions ("labile" P according to Negassa and Leinweber, 1996) increased rapidly, peaking after 2 weeks and then slowly decreasing. The proportions of the ^{33}P activity in the moderately labile, NaOH-extractable P pools showed the opposite trend: a slight decrease soon after fertilizer application with a minimum after two weeks of incubation, followed by a slight increase ($p < 0.05$). The stable fraction did not follow a pronounced temporal pattern (Figure 3; Supplementary Information, Table S1).

3.3 ^{33}P imaging

Autoradiographic imaging enabled qualitative tracing of ^{33}P released from the fertilizers within the Cambisol soil and plants (Figure 4). Images on the left-hand side of Figure 4 demonstrate that after one week of incubation a large proportion of the applied ^{33}P still occupied a layer at the soil surface where the NPK fertilizer and algal biomass were applied. This NPK fertilizer layer was slightly broader than that of the algal fertilizer treatment, indicating increased mobility, most likely due to the larger proportion of labile ^{33}P (the Resin-P pool) in the Cambisol also visible in Figure 3. A slight infiltration of the fertilizers also occurred at the rhizotron sidewalls, revealed by vertical streaks of radioactivity (Figure 4). However, there was no apparent leaching of ^{33}P through the soil matrix in the course of plant growth, from either the NPK or the algal fertilizer. A small amount of ^{33}P radioactivity was visible in the wheat shoots after the first week.

After three and six weeks of incubation, respectively, similar patterns were observed for both fertilizer forms (images on the right-hand site of Figure 4): ^{33}P was clearly detectable in all above-ground wheat shoots. This finding suggests that comparable amounts of radioactivity were taken up by the wheat plants from both types of fertilizer. Radioactivity was evenly distributed within the shoots. This ^{33}P accumulation in leaves occurred at the expense of fertilizer layers at

351 the soil surface that became much weaker compared to images that were taken after the first
352 week of incubation. Remarkably, visible ^{33}P activity was also detected in the roots. Again, no
353 visually noticeable differences in the roots between NPK and algae fertilization could be
354 observed.
355
356 **4 Discussion**
357 **4.1 Algae P release kinetics affected by soil group**
358 The higher ^{33}P activities in the labile P fraction of the Cambisol and Vertisol after mineral
359 fertilizer dissolution is caused by the high solubility of TSP (e.g., Siebers et al., 2012, Vogel et
360 al., 2017). The main component of TSP is $Ca(H_2PO_4)_2$, which has a high solubility (Kolay,
361 2007). This is different for the algae treatment, as *Chlorella vulgaris* stores P as complex
362 compounds in cells as a P reservoir (e.g., Eixler et al., 2006, Rao et al., 2009). The experiments
363 depicted in Figures 1 and 2 show that it is possible to prepare algal biomass in which P is
364 incorporated largely in the form of Poly-P granules or, as done here for the soil incubation and
365 rhizotron experiments, with Poly-P already largely converted to other biochemical compounds
366 containing P. In any case, the organic P compounds have to be mineralized before being plant-
367 available.
368 Due to their lower total Fe contents, the readily released P of the NPK fertilizer may remain in
369 easily-extractable, i.e., bioavailable forms in the Cambisol and Vertisol. The situation is different
370 in the Andosol and Alisol. As with other tropical and subtropical soils, these soils are highly
371 weathered and exhibit elevated contents of Fe/Al-oxides combined with lower pH values (Table
372 1). While initial release of P from NPK and algae likely occurred at similar rates, the distribution
373 of the released mineral P is thus increasingly superimposed by a contemporaneous sorption at
374 and fixation of the dissolved P by the oxidic soil matrix (Dahlgren et al., 2004; McGroddy et al.,

2008; Takeda et al., 2009; Fink et al., 2016). In addition, the high Al_{ox} content and the low pH value of the Andosol favor the precipitation of P with Al^{3+}, resulting in mineral phases such as variscite (Veith and Sposito, 1977), the formation of which additionally reduces P availability.

The high initial proportions of HCl- and aqua-regia extractable, i.e., stable P (Table 1; Negassa and Leinweber, 1996) in these soils confirm these fixation processes and are in agreement with earlier findings stating that stable P generally comprises >30% of the stable P fraction in moderately weathered soils and >80% of the stable P fraction in soils that are strongly weathered or derived from volcanic parent material (Condron and Newman, 2011; Turner et al., 2005). Nevertheless, we barely detected ^{33}P in these Residual-P pools (Figure 3), possibly reflecting limited transfer into these residual pools during the short incubation time of 10 weeks. Bauke et al. (2018) argued that "although surplus P from fertilizers may remain available in the short to medium term, it will eventually be transformed to unavailable forms of P over a period of a few decades", which was also suggested by Koch et al. (2018) detecting increased Residual-P concentrations after long-term compost fertilization.

By contrast to the stable P pools, P forms that are more easily extracted showed a temporal dynamics. Particularly the peak of labile P after 2 weeks of incubation is accompanied by a nadir of the proportions of moderately labile P fraction (Figure 3) and thus also for the respective total ^{33}P activity (Table S1, Table S2) as well as for the proportions (Figure 3). The moderately labile P fraction dynamics are fast and this fraction is still in equilibrium with the labile P fraction (Negassa and Leinweber, 2009). Thus, increasing moderately labile P observed after two weeks reflects the shift of the labile P fraction to more stable forms.

It is remarkable that 35-55% of algal-P can already be found in the labile P fraction after only one week of incubation in the Cambisol and Vertisol. This indicates that algal P is readily usable after microbial degradation of the cell wall of *Chlorella vulgaris*. The phospholipids present in

399 cell membranes as well as sugar-phosphates are rapidly degraded within seconds to minutes after
400 cell lysis (White et al., 1993, Siebers et al., 2015). This degradation likely involves phosphatases.
401 According to Hui et al. (2013), phosphatases operate at the scale of minutes to hours, similar to
402 pyrophosphates, which also potentially release orthophosphate within several hours (von Sperber
403 et al., 2016). The remaining P that is released less rapidly likely originates from that stored in
404 DNA/RNA, the degradation of which is further slowed when the DNA/RNA released after cell
405 lysis is bound to the soil matrix (Keown et al., 2005).
406
407 **4.2 Algae-P uptake by plants**
408 The overexpression of ^{33}P activity observed in the imager during the first weeks of the
409 experiment, using only 4 h of exposure, was caused by the high amount of ^{33}P initially applied to
410 the rhizotrons, which was necessary to account for its half-life of 25.6 days, shorter than the
411 growth period of the plants of 6 weeks. ^{33}P autoradiography demonstrated that algal P was being
412 taken up by plants one week after fertilizer application at a rate visually comparable that of NPK
413 fertilizer. Thus the results of our rhizotron experiments support the findings from our soil
414 incubation experiments that algae decomposition was rapid and increased the labile P fraction in
415 the Cambisol, if at a slightly lower rate than that provided by the NPK fertilizer. They also
416 support the findings from a previous study showing that algal-P is available to plants (Schreiber
417 et al., 2018).
418 In contrast to the incubation experiments the algal biomass in the fertilizer experiments was not
419 dried but applied intact in order simulate practice-orientated conditions as a pre-treatment. The
420 results nevertheless clearly showed that P from fresh, living algae (applied as a suspension in
421 water) was quickly mineralized and taken up by wheat roots. We therefore conclude that in
422 practice algal biomass does not need to be dried and granulated prior to application as a fertilizer,

423 saving energy costs. Instead, application of algal biomass jointly with liquid manure or using a
424 slurry applicator appears feasible at minimal extra costs. The combined application with a
425 grubber should allow a direct incorporation into soil, which in turn minimizes wind erosion. If
426 slower mineralization is desired (e.g., for perennial or more time-intensive cultures) granulation
427 of algal biomass will likely delay mineralization.
428
429 **4. Conclusion**
430 In the soils under study, P release from algal biomass was rapid and increased the concentrations
431 of labile and moderately labile P fractions in soil in a pattern comparable to that of mineral
432 fertilizer, although at a rate 1-9% lower than P release from NPK. These findings thus support
433 our two hypotheses that *Chlorella vulgaris* is capable of incorporating sufficient P into its
434 biomass to act as P fertilizer, releasing P when incorporated into the soil to support or even
435 sustain plant nutrition. Future work should now be performed to bring this fertilizer into the field
436 under economically viable, practice-relevant conditions.
437
438 **Acknowledgments**
439 The authors thank Christina Schreiber for helpful hints to algae growth and labeling. In addition,
440 we thank Meike Siebers and Peter Narf for valuable input regarding data interpretation. We also
441 thank Andrea Ecker for helping with ^{33}P analyses. This research was financially supported by the
442 Bioeconomy Science Center (BioSC) AlgalFertilizer and AlgalNutrient projects funded by the
443 Ministry of Innovation, Science and Research of the German State of North Rhine-Westphalia
444 (No. 313/323-400-002 13).
445
446 **Declaration of authors contributions**

NS, DH, NDJ, LN, and WA inspired the project AlgalFertilizer that provided partial funding for this research. LN inspired the project AlgalNutrient that also provided partial funding for this research. BA and LN conducted the experiments and analyzed the data leading to Fig. 1. LG and PM conducted experiments involving Raman microscopy and analyzed the data leading to Fig. 2. NS, HS, AL, and WA designed and conducted the soil incubation experiment and analyzed the data leading to Tab. 1 and Fig. 3. NS, DH, HS, BA, and WA conducted the experiments for ^{33}P algae labeling and rhizotron experiments and analyzed the data leading to Fig. 4. NS, DH, HS, and WA wrote the paper. All authors contributed to the revision of the paper draft.

Statement of Informed Consent, Human/Animal Rights

No conflicts, informed consent, human or animal rights applicable

References

Afi, L., Metzger, P., Largeau, C., Connan, J., Berkaloff, C., Rousseau, B. 1996. Bacterial degradation of green microalgae: Incubation of Chlorella emersonii and Chlorella vulgaris with Pseudomonas oleovorans and Flavobacterium aquatile. Organic Geochemistry. 25: 117–130.

Aslan, S., Ilgi, K.K. 2006. Batch kinetics of nitrogen and phosphorus removal from synthetic wastewater by algae. Ecological Engineering. 28: 64-70.

Bauke, S.L., von Sperber, C., Tamburini, F., Gocke, M.I., Honermeier, B., Schweitzer, K., Baumecker, M., Don, A., Sandhage-Hofmann, A., Amelung, W. 2018. Subsoil phosphorus is affected by fertilization regime in long-term agricultural experimental trials. European Journal of Soil Science. 69: 103-112.

Bauke, S.L., Landl, M., Koch, M., Hofmann, D., Nagel, K.A., Siebers, N., Schnepf, A., Amelung, W. 2017. Macropore effects on phosphorus acquisition by wheat roots – a rhizotron study. Plant and Soil. 416: 67–82.

Brányiková, I., Maršálková, B., Doucha, J., Brányik, T., Bišová, K., Zachleder, V., Vítová, M. 2011. Microalgae—novel highly efficient starch producers. Biotechnology and bioengineering. 108: 766-776.

Brown, N., A. Shilton. 2014. Luxury uptake of phosphorus by microalgae in waste stabilisation ponds: current understanding and future direction. Reviews in Environmental Science and Bio/Technology. 13.3: 321-328.

Condron, L.M., Newman, S. 2011. Revisting the fundamentals of phosphorus fractionation of sediments and soils. Soils Sediments. 11: 830–840.

481 Dahlgren, R.A., Saigusa, M., Ugolini, F.C. 2004. The Nature, Properties and Management of
482 Volcanic Soils, in: Advances in Agronomy, vol. 82. Elsevier, pp. 113–182.
483 Eixler, S., Karsten, U., Selig, U. 2006. Phosphorus storage in Chlorella vulgaris
484 (Trebouxiophyceae, Chlorophyta) cells and its dependence on phosphate supply.
485 Phycologia: 45: 53-60.
486 Fink, J.R., Inda, A.V., Tiecher, T., Barrón, V. 2016. Iron oxides and organic matter on soil
487 phosphorus availability. Ciênc. Agrotechnology. 40: 369–379.
488 Fleurence, J. 1999. The enzymatic degradation of algal cell walls: a useful approach for
489 improving protein accessibility? Journal of Applied Phycology. 11: 313–314.
490 Gerken, H.G., Donohoe, B., Knoshaug, E.P. 2013. Enzymatic cell wall degradation of Chlorella
491 vulgaris and other microalgae for biofuels production. Planta 237: 239–253.
492 Hedley, M.J., Stewart, J.W.B., Chauhan, B.S. 1982. Changes in Inorganic and Organic Soil
493 Phosphorus Fractions Induced by Cultivation Practices and by Laboratory Incubations.
494 Soil Science Society of America Journal. 46: 970.
495 Hui, D., Mayes, M.A., Wang, G. 2013. Kinetic parameters of phosphatase: A quantitative
496 synthesis. Soil Biology & Biochemistry. 65: 105-113.
497 Keown, H., Callaghan, O.M., Greenfield, L.C. 2004. Decomposition of nucleic acids in soil.
498 New Zealand Natural Sciences. 29: 13.
499 Koch, M., Kruse, J., Eichler-Löbermann, B., Zimmer, D., Willbold, S., Leinweber, P., Siebers,
500 N. 2018. Phosphorus stocks and speciation in a soil profile of a long-term fertilizer
501 experiment: evidence from sequential fractionation, ^{31}P-NMR, and P K-edge XANES
502 spectroscopy. Geoderma, 316: 115-126.
503 Kolay, A.K. 2007. Manures and fertilizer. Atlantic Publ. Distrib., New Delhi.
504 Lehndorff, E., Houtermans, M., Winkler, P., Kaiser, K., Kölbl, A., Romani, M., Said-Pullicino,
505 D., Utami, S.R., Zhang, G.L., Cao, Z.H., Mikutta, R., Guggenberger, G., Amelung, W.
506 2016. Black carbon and black nitrogen storage under long-term paddy and non-paddy
507 management in major reference soil groups. Geoderma. 284: 214-225.
508 Mainstone, C.P., Parr, W. 2002. Phosphorus in rivers — ecology and management. Science of
509 The Total Environment. 282-283: 25–47.
510 McBeath, T., Lombi, E., McLaughlin, M.J., Bünemann, E.K. 2007. Polyphosphate-fertilizer
511 solution stability with time, temperature, and pH. Journal of Plant Nutrition and Soil
512 Science. 170: 387-391.
513 McGroddy, M.E., Silver, W.L., Oliveira, R.C. de, Mello, W.Z. de, Keller, M. 2008. Retention of
514 phosphorus in highly weathered soils under a lowland Amazonian forest ecosystem.
515 Journal Geophysical Research. 113: 289–300.
516 Mertens, M.F., Pätzold, S., Welp, G. 2008. Spatial heterogeneity of soil properties and its
517 mapping with apparent electrical conductivity. Journal of Plant Nutrition and Soil Science.
518 171: 146–154.
519 Moudříková, Š., Mojzeš, P., Zachleder, V., Pfaff, C., Behrendt, D., Nedbal, L. 2016. Raman and
520 fluorescence microscopy sensing energy-transducing and energy-storing structures in
521 microalgae. Algal Research. 16:224-232.
522 Moudříková, Š., Sadowsky, A., Metzger, S., Nedbal, L., Mettler-Altmann, T., Mojzeš, P. 2017.
523 Quantification of polyphosphate in microalgae by Raman microscopy and by a reference
524 enzymatic assay. Analytical Chemistry. 89:12006-12013.
525 Nedbal, L., Trtílek, M., Červený, J., Komárek, O., & Pakrasi, H.B. 2008. A photobioreactor
526 system for precision cultivation of photoautotrophic microorganisms and for high content
527 analysis of suspension dynamics. Biotechnology and Bioengineering. 100: 902-910.

Negassa, W., Leinweber, P. 2009. How does the Hedley sequential phosphorus fractionation reflect impacts of land use and management on soil phosphorus: a review. Journal of Plant Nutrition and Soil Science. 172: 305–325.

Nishikawa, K., Machida, H., Yamakoshi, Y., Ohtomo, R., Saito, K., Saito, M., Tominaga, N., 2006. Polyphosphate metabolism in an acidophilic alga Chlamydomonas acidophila KT-1 (Chlorophyta) under phosphate stress. Plant Science. 170: 307–313.

Obersteiner, M., Peñuelas, J., Ciais, P., van der Velde, M., Janssens, I.A. 2013. The phosphorus trilemma. Nature Geoscience. 6: 897–898.

Powell, N., Shilton, A., Chisti, Y., Pratt, S. 2009. Towards a luxury uptake process via microalgae--defining the polyphosphate dynamics. Water Research. 43: 4207–4213.

Rao, N.N., Gómez-García, M.R., Kornberg, A. 2009. Inorganic polyphosphate: essential for growth and survival. Annual Review of Biochemistry. 78: 605–647.

Reijnders, L. 2014. Phosphorus resources, their depletion and conservation, a review. Resources, Conservation and Recycling. 93: 32–49.

Ruiz, J., Alvarez, P., Arbib, Z., Garrido, C., Barragán, J., Perales, J.A. 2011. Effect of nitrogen and phosphorus concentration on their removal kinetic in treated urban wastewater by Chlorella vulgaris. International Journal of Phytoremediation. 13: 884–896.

Schreiber, C., Schiedung, H., Harrison, L., Briese, C., Ackermann, B., Kant, J., Schrey, S.D., Hofmann, D., Singh, D., Ebenhöh, O., Amelung, W., Schurr, U., Mettler-Altmann, T., Huber, G., Jablonowski, N.D., Nedbal, L. 2018. Evaluating potential of green alga Chlorella vulgaris to accumulate phosphorus and to fertilize nutrient-poor soil substrates for crop plants. Journal of Applied Phycology. 30: 2827-2836.

Scholz, R.W., Ulrich, A.E., Eilitta, M., Roy, A. 2013. Sustainable use of phosphorus: a finite resource. Science of the Total Environment. 461-462: 799–803.

Siebers, M., Dörmann, P., & Hölzl, G. 2015. Membrane remodelling in phosphorus-deficient plants. Annual Plant Reviews. 48: 237-263.

Siebers, N., Godlinski, F., Leinweber, P. 2012. The phosphorus fertilizer value of bone char for potatoes, wheat, and onions: First results. Landbauforschung Volkenrode, 62: 59-64.

Solovchenko, A., Verschoor, A.M., Jablonowski, N.D., Nedbal, L. 2016. Phosphorus from wastewater to crops: An alternative path involving microalgae. Biotechnology Advances. 34: 550–564.

Stewart, W.D. (Ed.), 1974. Algal physiology and biochemistry. Botanical monographs 10. Univ. of California Press, Berkeley Calif. u.a., XI, 989 S.

Takeda, M., Nakamoto, T., Miyazawa, K., Murayama, T., Okada, H. 2009. Phosphorus availability and soil biological activity in an Andosol under compost application and winter cover cropping. Applied Soil Ecology. 42: 86–95.

Turner, B.L., Cade-Menun, B.J., Condron, L.M., Newman, S. 2005. Extraction of soil organic phosphorus. Talanta. 66: 294–306.

Vaccari, D.A. 2009. Phosphorus: A Looming Crisis. Scientific American. 300: 54–59.

Veith, J.A., Sposito, G. 1977. Reactions of Aluminosilicates, Aluminum Hydrous Oxides, and Aluminum Oxide with o-Phosphate: The Formation of X-ray Amorphous Analogs of Variscite and Montebrasite. Soil Science Society of America Journal. 41: 870-876.

Vogel, T., Kruse, J., Siebers, N., Nelles, M., Eichler-Löbermann, B. 2017. Recycled products from municipal waste water: Composition and effects on phosphorus mobility in a sandy soil. Journal of Environmental Quality. 46: 443-451.

von Sperber, C., Lewandowski, H., Tamburini, F., Bernasconi, S.M., Amelung, W., Frossard, E. 2016. Kinetics of pyrophosphatase catalyzed oxygen isotope exchange between phosphate and water revealed by Raman spectroscopy. Journal Raman Spectroscopy. 48: 368-373.

Wallmann, K. 2010. Phosphorus imbalance in the global ocean? Global Biogeochemistry Cycles. 24(4).

White, D.C., Meadows, P., Eglinton, G., Coleman, M.L. 1993. In situ measurement of microbial biomass, community structure and nutritional status [and discussion]. Philosophical Transactions of the Royal Society A: Mathematical, Physical and Engineering Sciences. 344: 59–67.

Whitton, R., Le Mevel, A., Pidou, M., Ometto, F., Villa, R., Jefferson, B. 2016. Influence of microalgal N and P composition on wastewater nutrient remediation. Water Research. 91: 371–378.

Winkler, P., Kaiser, K., Kölbl, A., Kühn, T., Schad, P., Urbanski, L., Fiedler, S., Lehndorff, E., Kalbitz, K., Utami, S.R., Cao, Z., Zhang, G., Jahn, R., Kögel-Knabner, I. 2016. Response of Vertisols, Andosols, and Alisols to paddy management. Geoderma. 261: 23-35.

WRB. 2015. World reference base for soil resources 2014, update 2015: International soil classification system for naming soils and creating legends for soil maps.

591 **Tables**

592

593 **Table 1**. General soil characteristics of the soils used; Al_{ox}, Fe_t, $Fe_{DCB}/_{Fet}$, and Fe_{ox}/Fe_{DCB} data
594 were obtained from Winkler et al. (2016) for the Vertisol, Andosol, and Alisol being the same
595 soil samples as used in this study. Phosphorus fractions determined using sequential fractionation
596 for the different soils studied with proportions of total P (P_t) in parentheses. (Data are shown as
597 mean ± standard deviation (SD), n=3).

	Cambisol	Andosol	Alisol	Vertisol
Soil	Orthic Cambisol	Dystric silandic Andosol	Chromic abruptic Alisol	Pellic Vertisol
pH ($CaCl_2$)	5.9±0.0	4.6±0.0	4.9±0.0	5.7±0.0
Sand (%)	23.9±0.9	76.3±0.0	10.4±0.0	5.6±0.0
Silt (%)	58.1±0.5	23.7±0.6	19.6±0.0	20.8±0.2
Clay (%)	14.9±0.3	3.9±0.1	71.5±0.4	77.3±0.2
SOC (%)	1.90±0.03	2.37±0.01	1.62±0.08	1.30±0.07
N (%)	0.18±0.00	0.27±0.00	0.17±0.01	0.1±0.00
C/N	10.4	8.9	9.8	12.6
Al_{ox} (g kg^{-1})	< 0.4	2.9±0.2	< 0.4	< 0.4
Fe_t (g kg^{-1})	19.0±0.5	96.4±1.4	85.8±2.1	68.5±1.3
Fe_{DCB}/Fe_t	0.41	0.44	0.67	0.09
Fe_{ox}/Fe_{DCB}	0.50	0.38	0.06	0.58
Resin-P	92±1.9 (6)	3.0±2.2 (0)	3.2±0.3 (0)	19±0.5 (5)
$NaHCO_3$-Pi (mg kg^{-1})	86±0.8 (6)	30±0.2 (1)	11±1.0 (1)	11±0.2 (3)
$NaHCO_3$-Po (mg kg^{-1})	245±0.8 (16)	10±2.6 (0)	11±1.4 (1)	12± 0.5 (3)
NaOH-Pi (mg kg^{-1})	275±14.9 (18)	803±12 (32)	149±46 (17)	35±0.2 (9)
NaOH-Po (mg kg^{-1})	95±24.5 (6)	499±54 (20)	76±2.5 (8)	6.9±0.6 (2)
HCl-Pi (mg kg^{-1})	133±2.0 (7)	44±1.2 (2)	5.1±1.1 (1)	23±0.6 (5)
HCl-Po (mg kg^{-1})	11±2.8 (1)	69±0.0 (3)	8.8±1.3 (1)	12±1.0 (3)
Residual-P (mg kg^{-1})	603±15.2 (39)	1070±91 (42)	642 ± 8.0 (71)	286±125 (70)
P_t (mg kg^{-1})	1540±79	2528±204	906±77	405 ±16

598

599

Figures

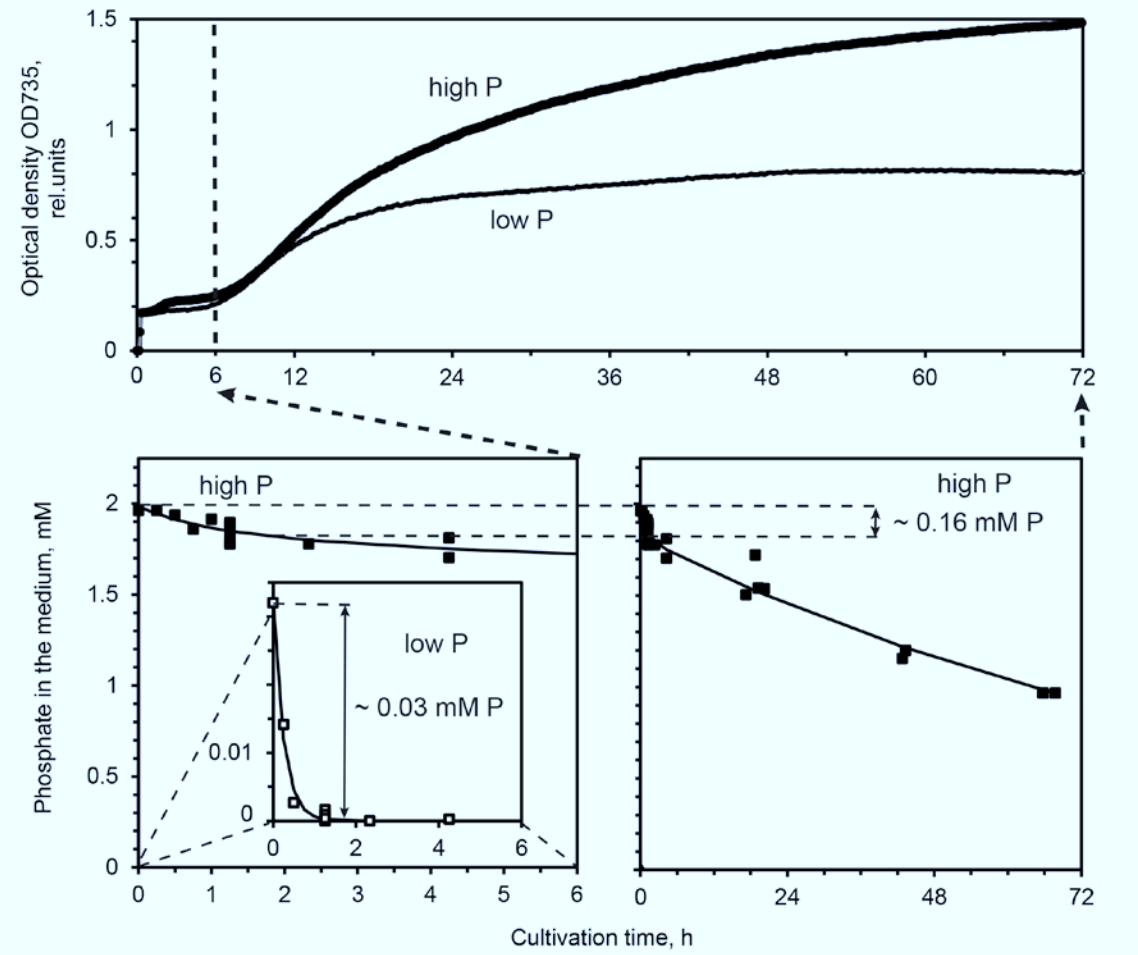

Figure 1. The upper panel shows growth approximated by optical densities of *Chlorella vulgaris* C1 after P-starved cultures were added into a high-P medium with 2 mM KH_2PO_4 (thick line) and into low-P medium with 0.03 mM KH_2PO_4 (thin line). The maximal specific growth rate was 0.21 h^{-1} in the high-P medium and 0.14 h^{-1} in the low-P medium. The lower panels show dynamics of phosphate in the respective medium: 2 mM KH_2PO_4 (full squares) and 0.03 mM KH_2PO_4 (open squares). The curves approximate the uptake dynamics by numerical fits: 0.03 mM · exp(-time/0.25 h) for the low-P concentration and 0.16 mM exp(-time/1.1 h) + 1.8 mM · exp(-time/110 h) for the high-P concentration. Only the results of one experiment (n=1) are shown, as even though all five replicates yielded qualitatively identical results however variably long lag phases (between 4 to 8 hours, data not shown). Therefore, calculating the mean of all replicates would mix statistical and systematic deviations and obscure the basic biphasic character.

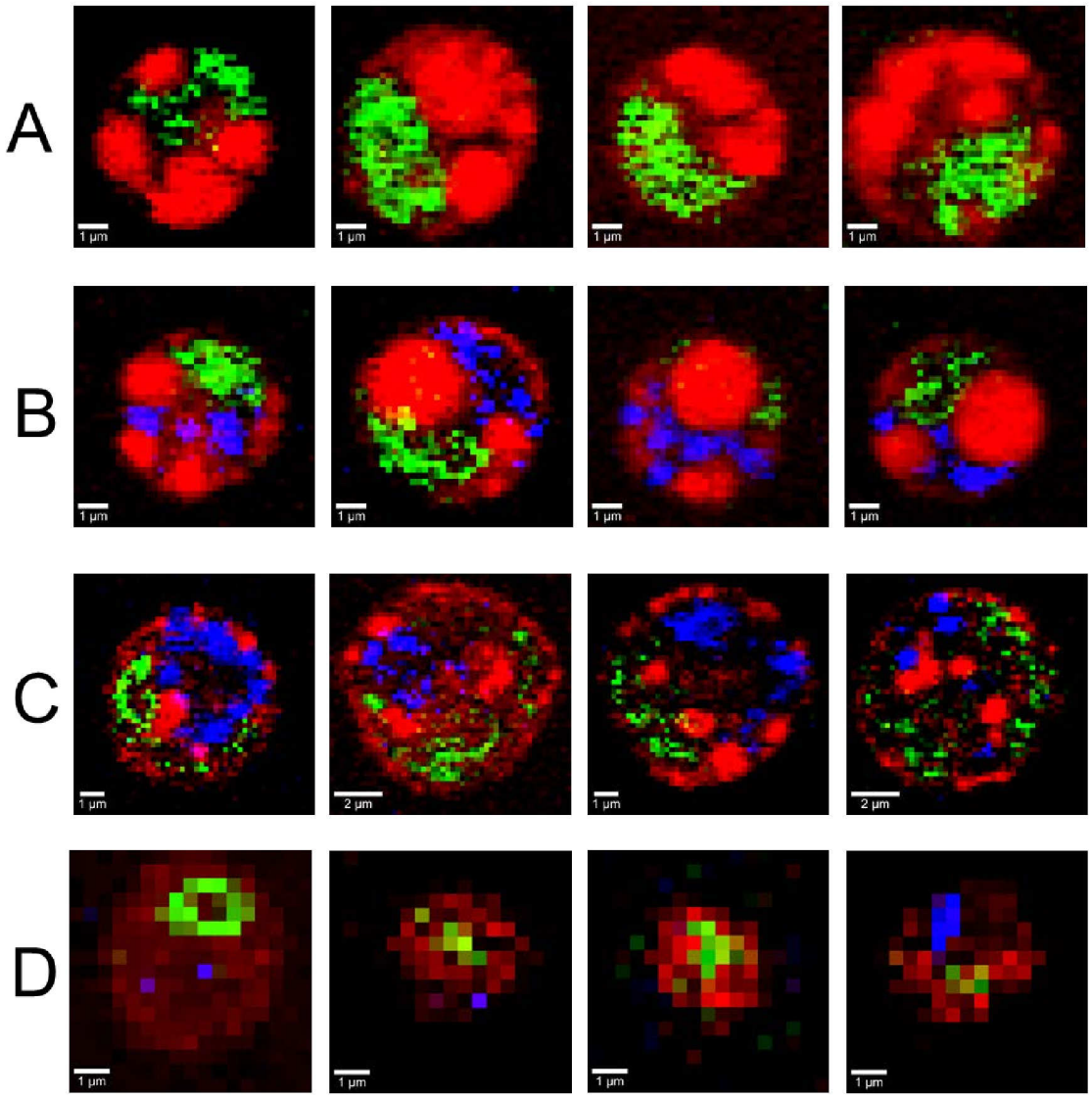

Figure 2. Raman images of four (n=4) cells *Chlorella vulgaris* CCALA256 representing the P-starved culture (row A), cells collected 2 h after adding 0.4 mM orthophosphate (row B), in early exponential phase (row C), and in rapidly growing and dividing cells (row D). The images represent Raman spectral signatures of neutral lipids (red) and of starch (green) that represent the major reserves of organic carbon while the blue color shows the Raman spectral signature of polyphosphates.

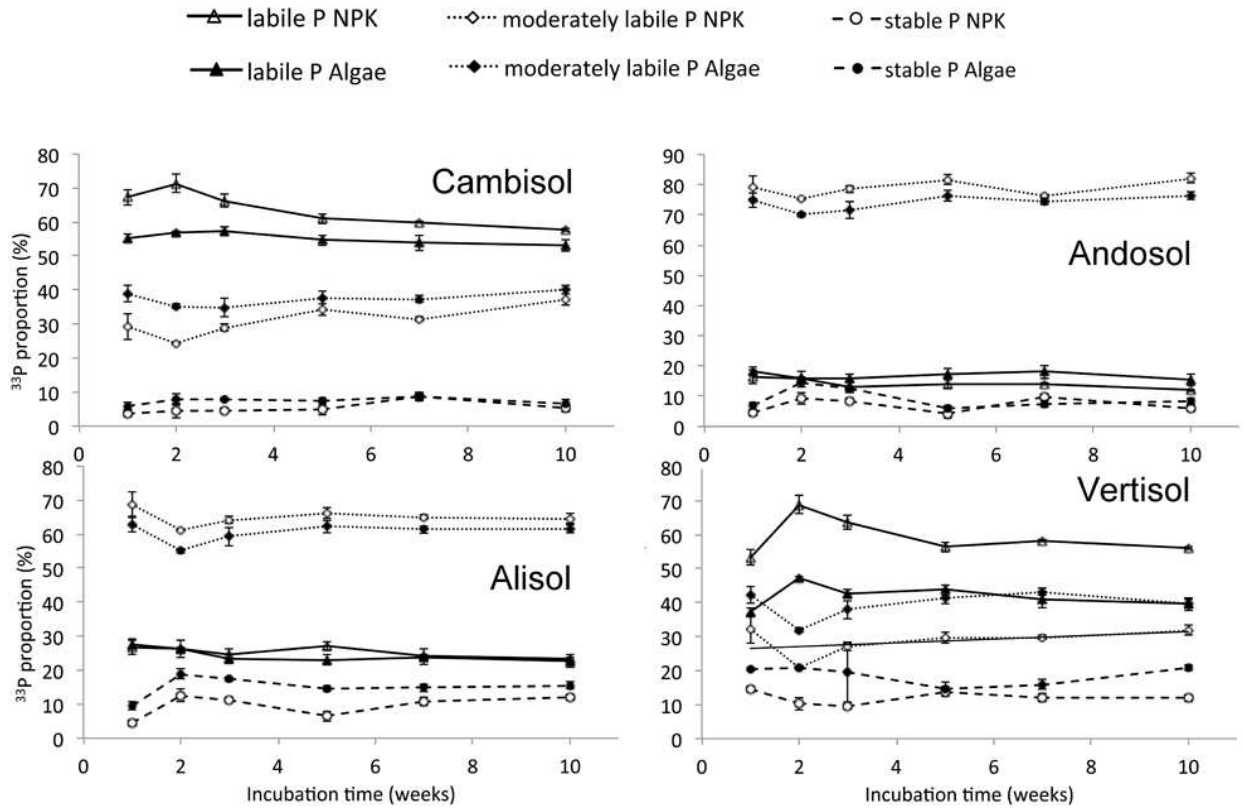

Figure 3. Development of ^{33}P activity in different P fractions, i.e., labile P comprising Resin-P and $NaHCO_3$-P, moderately labile P comprising NaOH-P, and stable P comprising HCl-P and Residual-P, throughout 10 weeks of incubation after NPK and algae fertilizer application. (Data are shown as mean ± standard deviation (SD), n=3).

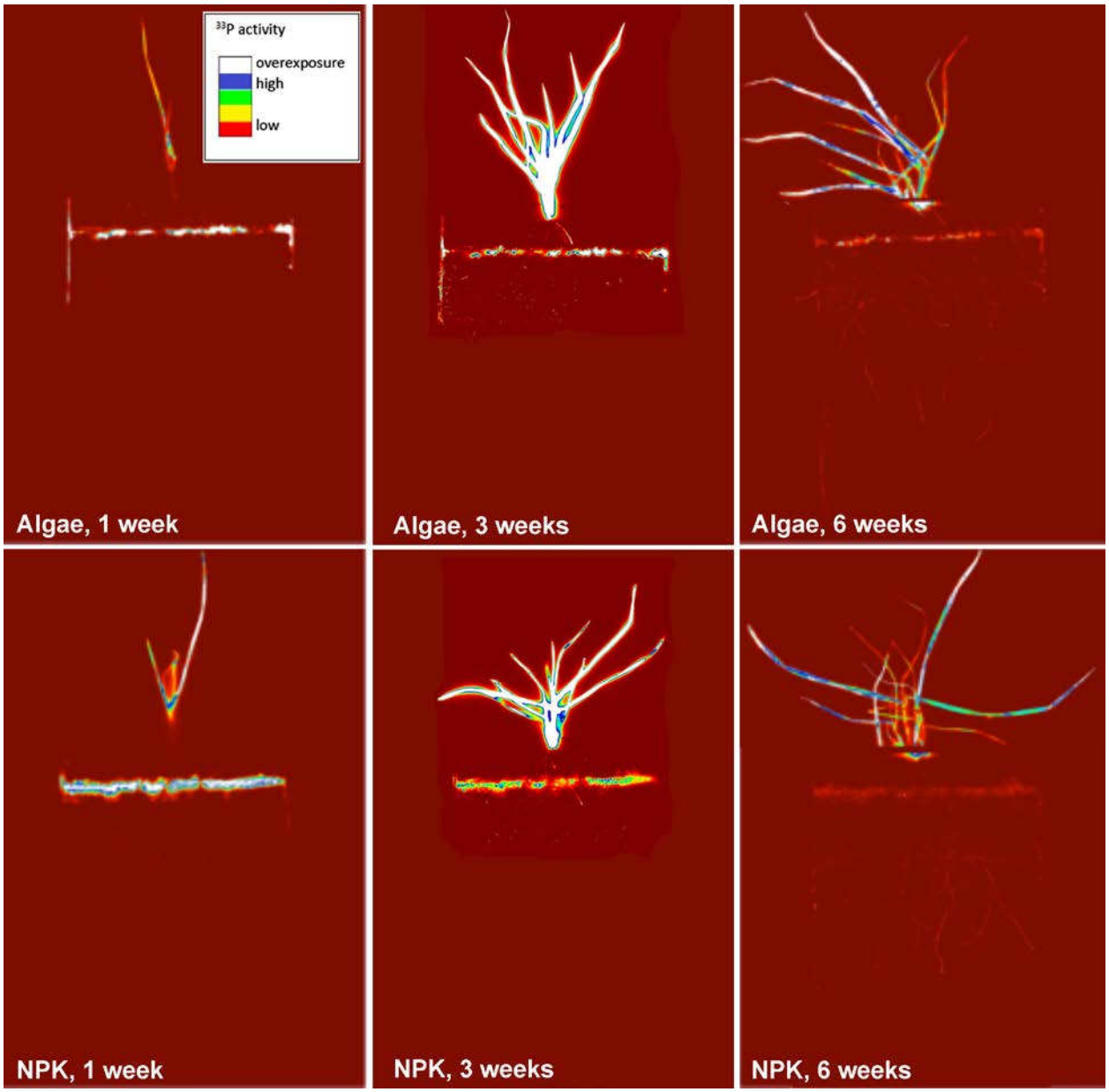

Figure 4. ^{33}P-autoradiographic images of rhizotrons with wheat plants after fertilization using previously labeled ^{33}P-labeled algae and ^{33}P-labeled mineral NPK fertilizer after one, three, and six weeks of growth. The exposure time of the image plates was 4 h; n=1.

SUPPLEMENTAL INFORMATION

Supplemental Table S1. The total ^{33}P activity of the soil for each week after NPK and Algae fertilization for each replicate.

Week	Fertilization	Cambisol	Andosol	Alisol	Vertisol
		$^{33}P_t$ (Bq g^{-1} soil)			
1	NPK	961	1573	2878	840
1		1007	1511	3576	1052
1		2925	1410	1963	1135
2		1113	1657	2844	1163
2		1027	1925	4715	1339
2		3221	1532	2839	1441
3		982	2013	3690	1792
3		1042	1960	4365	1961
3		2893	1526	2562	1031
5		951	1743	2970	788
5		850	1810	3834	924
5		2927	1496	2173	864
7		1049	1500	3110	1020
7		1049	1773	3769	1048
7		3171	1346	1949	1150
10		960	2034	3509	1195
10		911	2004	4190	1059
10		2717	1407	2249	1162
1	Algae	1056	3047	4407	610
1		2480	3157	3677	1371
1		3569	1851	4227	1492
2		1385	3779	6237	894
2		2491	2934	6525	1737
2		4269	2147	5858	2054
3		1223	4038	4341	793
3		2614	3044	5731	1738
3		4367	2134	5279	2027
5		1316	3635	5140	693
5		2328	2815	5036	3453
5		3893	1882	5370	3461
7		2146	3494	4244	840
7		2438	2809	4573	2098
7		3902	1615	3955	2378
10		1430	4134	4493	493
10		2662	2991	6086	1694
10		4291	1882	4219	2233

Supplemental Table S2. The ^{33}P activity proportions as related to total ^{33}P in each fractions as determined by sequential extraction. Different lowercase letters indicate significant differences with incubation time, whereas different uppercase letters indicate significant differences between NPK and Algae fertilizer at given incubation week. (Data are shown as mean ± standard deviation (SD), n=3).

Week	Fertilization	Resin-P	$NaHCO_3$-P	NaOH-P	HCl-P	Residual-P
		Proportions (%)				
Cambisol 1	NPK	30.1±0.4^{aA}	37.0±1.2^{aA}	29.2±1.1^{aA}	2.7±0.2^{aA}	0.8±0.6^{aA}
2	NPK	41.9±0.9^{bA}	29.5±1.5^{bA}	24.4±0.3^{bA}	3.0±0.2^{aA}	1.3±0.5^{aA}
3	NPK	32.9±1.5^{cA}	33.4±0.5^{cA}	29.0±0.8^{acA}	3.6±0.4^{aA}	1.1±0.1^{aA}
5	NPK	24.7±1.3^{dA}	36.3±0.8^{acA}	34.2±0.6^{dA}	4.3±0.1^{aA}	0.6±0.4^{aA}
7	NPK	25.9±0.7^{edA}	34.1±1.2^{acA}	31.4±0.1^{eA}	3.3±0.2^{aA}	5.2±1.7^{bA}
10	NPK	29.9±0.7^{faA}	27.8±1.0^{bA}	37.1±0.8^{fA}	4.1±0.1^{aA}	1.1±0.2^{aA}
1	Algae	21.0±2.0^{aB}	34.2±1.7^{aB}	38.9±1.9^{abB}	4.3±0.5^{aB}	1.6±0.3^{aA}
2	Algae	32.5±0.6^{bB}	24.3±2.4^{bB}	35.2±2.5^{aB}	3.6±0.2^{aB}	4.4±0.4^{bB}
3	Algae	27.1±0.9^{cB}	30.4±0.3^{aB}	34.8±1.4^{aB}	4.1±0.3^{aA}	3.7±0.3^{bB}
5	Algae	22.2±0.6^{aB}	32.5±0.5^{aB}	37.7±1.3^{abB}	4.2±0.6^{aA}	3.4±0.2^{bB}
7	Algae	21.6±1.3^{aB}	32.3±3.3^{aA}	37.3±0.2^{abB}	5.8±3.4^{aA}	3.0±1.0^{bcA}
10	Algae	23.0±1.6^{aB}	30.1±1.9^{aA}	40.1±1.1^{bB}	4.4±0.8^{aA}	2.4±0.1^{cB}
Andosol 1	NPK	0.5±0.2^{aA}	15.8±1.3^{abA}	79.2±0.8^{aA}	2.0±0.4^{aA}	2.5±0.5^{aA}
2	NPK	1.3±0.0^{bcA}	14.4±0.4^{bA}	75.2±0.6^{bA}	2.1±0.1^{aA}	7.0±0.5^{bA}
3	NPK	1.0±0.2^{abcA}	12.0±0.0^{cA}	78.6±0.4^{acA}	2.1±0.5^{aA}	6.3±0.1^{bA}
5	NPK	0.9±0.1^{abcA}	13.1±0.6^{bcA}	81.7±1.1^{aA}	1.9±0.1^{aA}	2.4±1.1^{acA}
7	NPK	1.1±0.1^{cbA}	13.0±0.1^{bA}	76.3±1.5^{bcA}	2.0±0.2^{aA}	7.6±1.3^{bA}
10	NPK	1.1±0.2^{bcdA}	10.8±0.8^{cA}	82.2±1.1^{aA}	2.0±0.1^{aA}	3.9±0.4^{cA}
1	Algae	0.5±0.1^{aA}	17.9±2.3^{aA}	74.9±2.1^{abB}	1.5±0.1^{aA}	5.2±0.5^{aB}
2	Algae	0.6±0.1^{abB}	15.1±2.1^{aA}	70.0±2.8^{aB}	1.7±0.2^{aA}	12.6±1.1^{bB}
3	Algae	0.5±0.0^{acB}	15.5±0.4^{aB}	71.6±0.6^{abcB}	1.9±0.2^{aA}	10.6±0.5^{bB}
5	Algae	0.7±0.0^{beA}	16.8±0.6^{aB}	76.5±0.4^{bcB}	1.7±0.2^{aA}	4.3±0.8^{aA}
7	Algae	0.7±0.1^{beA}	17.3±0.6^{aB}	74.4±0.1^{abcA}	1.9±0.2^{aA}	5.6±0.4^{aA}
10	Algae	0.5±0.0^{abB}	14.9±1.2^{aB}	76.4±2.8^{cbB}	2.5±0.3^{bA}	5.7±1.6^{aA}
Alisol 1	NPK	4.2±0.9^{aA}	22.6±1.1^{aA}	68.7±1.1^{aA}	0.6±0.1^{aA}	3.9±0.3^{aA}
2	NPK	10.8±1.4^{bA}	15.5±0.4^{bA}	61.2±1.3^{bA}	0.7±0.1^{aA}	11.8±0.2^{bA}
3	NPK	8.7±0.8b^{cA}	15.7±0.6^{bcA}	64.2±0.8^{cA}	0.9±0.1^{aA}	10.5±0.9^{bA}
5	NPK	8.6±1.2b^{cA}	18.6±0.2^{dA}	66.3±0.7^{acA}	0.8±0.1^{aA}	5.7±0.9^{cA}
7	NPK	8.0±0.7^{cA}	16.3±0.8^{bcA}	65.0±0.7^{dA}	0.7±0.0^{aA}	10.1±2.0^{bA}
10	NPK	8.6±0.7^{bcA}	14.7±1.2^{bcA}	64.7±1.3^{cdA}	2.1±2.4^{aA}	9.9±1.3^{bA}
1	Algae	5.5±1.0^{aA}	22.0±0.9^{aA}	63.0±1.6^{aB}	0.6±0.2^{aA}	8.9±1.6^{aB}
2	Algae	8.5±0.6^{bA}	17.7±1.1^{bA}	55.0±1.4^{bB}	0.8±0.1^{aA}	18.1±0.9^{bB}
3	Algae	6.6±0.8^{abcA}	16.9±0.7^{bA}	59.3±1.0^{aB}	0.9±0.1^{aA}	16.4±0.4^{bcB}
5	Algae	6.2±0.6^{cA}	16.8±0.8^{bA}	62.3±0.7^{aB}	0.7±0.0^{aA}	13.9±0.4^{cdB}
7	Algae	6.6±0.4^{abcA}	17.3±0.6^{bA}	61.4±0.4^{aB}	0.9±0.0^{aA}	13.9±1.0^{cdB}
10	Algae	6.2±1.0^{acA}	16.5±1.2^{bA}	61.7±2.3^{aA}	1.0±0.1^{aA}	14.6±2.4^{bcB}
Vertisol 1	NPK	11.0±1.1^{aA}	42.4±2.2^{aA}	32.0±3.9^{aA}	10.5±2.0^{acA}	4.1±0.9^{aA}

	2	NPK	43.9±0.6^{bA}	25.0±0.9^{bA}	20.9±0.3^{bA}	7.5±0.6^{bA}	2.8±1.9^{aA}
	3	NPK	37.6±1.3^{bA}	26.0±0.8^{bA}	27.1±1.2^{aA}	7.6±1.0^{bA}	1.8±0.7^{aA}
	5	NPK	25.9±1.6^{cA}	30.4±1.2^{cA}	29.7±1.6^{aA}	12.4±0.2^{cA}	1.5±1.5^{aA}
	7	NPK	28.6±2.3^{cA}	29.6±0.9^{cA}	29.7±0.6^{aA}	9.8±0.3^{aA}	2.2±1.1^{aA}
	10	NPK	31.2±1.8^{dA}	25.0±1.1^{bA}	31.9±1.6^{aA}	9.3±0.7^{aA}	2.7±0.9^{aA}
	1	Algae	6.9±2.2^{aB}	30.5±4.6^{abB}	42.3±2.4^{aB}	9.0±0.6^{aA}	11.4±0.5^{aB}
	2	Algae	17.1±2.6^{bB}	30.1±1.5^{aB}	31.9±0.6^{bB}	8.0±0.2^{bA}	13.0±0.5^{aB}
	3	Algae	12.4±2.0^{cB}	30.2±3.9^{abA}	38.0±2.7^{aB}	9.1±2.0^{abA}	10.4±8.7^{aA}
	5	Algae	12.2±1.4^{cB}	31.6±3.0^{aA}	41.6±1.9^{aB}	9.4±0.2^{aB}	5.3±2.0^{aA}
	7	Algae	12.6±0.3^{cB}	28.3±0.4^{abA}	43.2±1.1^{aB}	9.4±0.7^{aA}	6.6±1.5^{aB}
	10	Algae	11.9±0.4^{cB}	27.7±0.4^{bA}	39.6±1.3^{aB}	11.7±0.2^{cB}	9.2±0.7^{aB}

646